

On the attribution of changing pan evaporation

Michael L. Roderick,¹ Leon D. Rotstayn,² Graham D. Farquhar,¹ and Michael T. Hobbins¹

Received 17 July 2007; revised 17 July 2007; accepted 8 August 2007; published 13 September 2007.

[1] Evaporative demand, measured by pan evaporation, has declined in many regions over the last several decades. It is important to understand why. Here we use a generic physical model based on mass and energy balances to attribute pan evaporation changes to changes in radiation, temperature, humidity and wind speed. We tested the approach at 41 Australian sites for the period 1975–2004. Changes in temperature and humidity regimes were generally too small to impact pan evaporation rates. The observed decreases in pan evaporation were mostly due to decreasing wind speed with some regional contributions from decreasing solar irradiance. Decreasing wind speeds of similar magnitude has been reported in the United States, China, the Tibetan Plateau and elsewhere. The pan evaporation record is invaluable in unraveling the aerodynamic and radiative drivers of the hydrologic cycle, and the attribution approach described here can be used for that purpose. **Citation:** Roderick, M. L., L. D. Rotstayn, G. D. Farquhar, and M. T. Hobbins (2007), On the attribution of changing pan evaporation, *Geophys. Res. Lett.*, *34*, L17403, doi:10.1029/2007GL031166.

1. Introduction

[2] Measurements of evaporation from pans have traditionally been used to represent the evaporative demand of the atmosphere when estimating crop water requirements [Doorenbos and Pruitt, 1977; Stanhill, 2002]. Averages over many pans show declines over the last 30 to 50 years with typical rates of -2 to -5 mm a⁻² (mm per annum per annum) reported in the USA and across many parts of the former Soviet Union [Peterson et al., 1995; Golubev et al., 2001; Groisman et al., 2004], China [Liu et al., 2004; Chen et al., 2005; Wu et al., 2006], Canada [Burn and Hesch, 2007], Australia [Roderick and Farquhar, 2004], New Zealand [Roderick and Farquhar, 2005] and on the Tibetan plateau [Shenbin et al., 2006; Zhang et al., 2007]. That range is not universal and data from India [Chattopadhyay and Hulme, 1997] and Thailand [Tebakari et al., 2005] show declines of -10 to -12 mm a⁻².

[3] Evaporation pans are useful in agro-ecology and hydrology because they are simple robust instruments that integrate the relevant physical factors, namely radiation, temperature, humidity and wind speed, into a single measure of evaporative demand. However, understanding the

observed decline in evaporative demand requires that integration be unraveled. Previous efforts to do this have been based on simplified arguments [Roderick and Farquhar, 2002] or calculations that assume a surface of short green grass [Thomas, 2000; Chen et al., 2005; Shenbin et al., 2006] instead of a pan. The preferred approach is to calculate pan evaporation using physical variables and we developed a generic model, called PenPan, for that purpose [Rotstayn et al., 2006]. Here we test the use of that model to attribute changes in pan evaporation to changes in the underlying physical variables.

2. Attribution Using the PenPan Model

[4] The PenPan model is based on Penman's combination equation [Penman, 1948]. It assumes a steady state energy balance, which for a Class A pan requires periods of at least a week and the applications described later use monthly input data. The radiative and aerodynamic components are based on the Linacre [1994] and Thom et al. [1981] models respectively. In brief, the evaporation rate from the pan (E_p , kg m⁻² s⁻¹) is expressed as the sum of radiative ($E_{p,R}$) and aerodynamic ($E_{p,A}$) components,

$$E_p = E_{p,R} + E_{p,A} = \left(\frac{s}{s + a\gamma} \frac{R_n}{\lambda} \right) + \left(\frac{a\gamma}{s + a\gamma} f_q(u) D \right) \quad (1)$$

with s (Pa K⁻¹) the change in saturation vapour pressure (e_s , Pa) with temperature evaluated at the air temperature (T_a , K) two metres above the ground, R_n (W m⁻²) the net irradiance of the pan, λ (J kg⁻¹) the latent heat of vaporisation, a ($= 2.4$ here) the ratio of effective surface areas for heat and vapour transfer, γ (~ 67 Pa K⁻¹) the psychrometric constant, D ($= e_s - e_a$, Pa) the vapour pressure deficit at two metres and $f_q(u)$ (kg m⁻² s⁻¹ Pa⁻¹) the vapour transfer function [Thom et al., 1981],

$$f_q(u) = 1.39 \times 10^{-8} (1 + 1.35 u) \quad (2)$$

where u (m s⁻¹) is the mean wind speed at two metres above the ground. The net irradiance of the pan is,

$$R_n = (1 - A_p) R_{sp} + R_{l,in} - R_{l,out} \quad (3)$$

The last two terms are the incoming ($R_{l,in}$) and outgoing ($R_{l,out}$) long-wave irradiance, with $R_{l,out}$ calculated assuming the pan is a black body radiating at temperature T_a . The first term is the net short-wave irradiance, with A_p ($= 0.14$ here) the pan albedo and R_{sp} the incoming short-wave irradiance of the pan. R_{sp} is greater than the global solar irradiance (R_s) because of additional interception by the walls of the pan [Rotstayn et al., 2006].

¹Cooperative Research Centre for Greenhouse Accounting, Environmental Biology Group, Research School of Biological Sciences, Australian National University, Canberra, ACT, Australia.

²Marine and Atmospheric Research, CSIRO, Aspendale, Victoria, Australia.

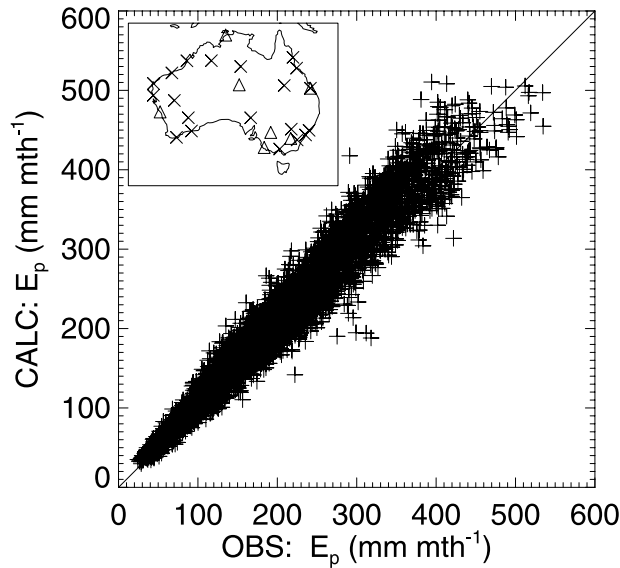


Figure 1. Comparison of observed and calculated pan evaporation rates. The PenPan model was forced with observations (R_s , T_a , e_s , e_a , u) with $R_{l,in}$ calculated using equation (6). Locations ($n = 26$ sites) shown in the inset where sites denoted Δ are the seven “elite” sites (listed in Table 1). Best fit regression; $y = 1.01x + 7.7$, $R^2 = 0.95$, $n = 5071$ (1:1 line shown). The RMSE is 24 mm mth^{-1} . (Note that $1 \text{ mm} = 1 \text{ kg m}^{-2}$.)

[5] For attribution, the change in pan evaporation rate is given by differentiating equation (1),

$$\frac{dE_p}{dt} = \frac{dE_{p,R}}{dt} + \frac{dE_{p,A}}{dt} \quad (4)$$

The term $dE_{p,A}/dt$ is then partitioned into three components, denoted U^* , D^* , T^* for changes due to changing wind speed, vapour pressure deficit and temperature respectively. The components are defined by,

$$\frac{dE_{p,A}}{dt} \approx \frac{\partial E_{p,A}}{\partial u} \frac{du}{dt} + \frac{\partial E_{p,A}}{\partial D} \frac{dD}{dt} + \frac{\partial E_{p,A}}{\partial s} \frac{ds}{dt} \frac{dT_a}{dt} = U^* + D^* + T^* \quad (5)$$

3. Materials and Methods

[6] Data were collated from existing Australian Bureau of Meteorology (BoM) digital records: class A pan evaporation and wind speed (IDCJDC05.200506), temperature and humidity (IDCJHC02.200506) and radiation (NCCSOL Vers 2.209). We estimated monthly averages when 25 daily observations were flagged as validated by the BoM. Months not satisfying this criterion were omitted. T_a and humidity was measured in Stevenson screens, while u was measured using an anemometer 2 m above the pan. Starting with the 60 or so high quality sites previously identified [Roderick and Farquhar, 2004; Jovanovic et al., 2005], we identified a

subset of 41 sites (auxiliary Table S1¹) having near-complete records of E_p and the observations needed to calculate $E_{p,A}$.

[7] As in many regions [Stanhill, 1997] the radiation database [Forgan, 2005] is the most heterogeneous of the meteorological databases. Of the 41 sites, 26 have some measurements of R_s (auxiliary Table S1) in the 1975–2004 period, but only seven have complete 30-year records. Observations of $R_{l,in}$ are more restrictive with 11 sites having observations, the earliest from 1995. For 1975–2004, we estimated $R_{l,in}$ at any site having R_s observations using the FAO56 approach [Allen et al., 1998],

$$R_{l,in} = \sigma T_a^4 \left(1 - \left(0.34 - 0.14 \sqrt{e_a/1000} \right) \cdot \left(1.35 R_s / (R_o (0.75 + 2 \times 10^{-5} z)) - 0.35 \right) \right) \quad (6)$$

with R_o (W m^{-2}) the top of atmosphere solar irradiance, and z (m) the site elevation. Equation (6) includes water vapour but ignores other greenhouse gases (e.g., CO_2) and aerosols (e.g., dust). For the 30-year period considered here, the effect of trends in the ignored greenhouse gases on $R_{l,in}$ should be small compared to the known trends in E_p . Further, recent simulations with the CSIRO climate model suggest that changes in dust-loading over Australia were also small between the 1950s and 1990s [Rotstayn et al., 2007].

[8] Digital metadata (BoM) showed no site location changes at any of the 41 sites. We examined the observations for obvious problems, especially discontinuities due to, for example, unreported changes in site location. At Darwin Airport, there was an obvious problem with u measurements before 1977 (auxiliary Figure S3). All analyses at that site are for 1977–2004. In several other instances, we identified what initially appeared to be suspect E_p observations. For example, at Alice Springs the very low E_p during 1975–1978 look anomalous when viewed in isolation. However, they were quantitatively consistent with the concurrent low values of u , D and R_s (auxiliary Figure S3). The same was found when examining other apparently anomalous situations.

4. Results

4.1. Evaluation of the PenPan Model

[9] We first used the PenPan model to calculate E_p using complete (post-1995) observations (R_s , $R_{l,in}$, T_a , u , e_s , e_a). The agreement between modelled and observed E_p at the 11 sites (auxiliary Figure S1, $R^2 = 0.95$, $n = 903$, RMSE = 22 mm mth^{-1}) was excellent. Next, we used the available $R_{l,in}$ observations to evaluate the FAO56 equation. There was no evidence of a change in the slight bias ($\sim 6 \text{ W m}^{-2}$) over time (results not shown) and we concluded that equation (6) was satisfactory for the intended purpose (auxiliary Figure S2, $R^2 = 0.97$, $n = 916$). Finally, we used equation (6) to estimate $R_{l,in}$ and thereby calculated E_p at the 26 sites for any month with observations of R_s , T_a , u , e_s and e_a . The comparison with E_p observations was excellent (Figure 1).

¹Auxiliary material data sets are available at <ftp://ftp.agu.org/apend/gl/2007gl031166>. Other auxiliary material files are in the HTML.

Table 1. Observed (OBS) and Model-Calculated (CALC) Trends in Pan Evaporation Rate (dE_p/dt , in mm a^{-2}) at 7 Sites Having Near-Continuous Data for 1975–2004^a

Site	OBS	CALC = Rad + Aero	Rad	Aero	Aero Partition		
	dE_p/dt	dE_p/dt	$dE_{p,R}/dt$	$dE_{p,A}/dt$	U^*	D^*	T^*
GERALDTON AIRPORT	-4.1	-2.2	0.0	-2.2	-1.6	-0.8	0.3
DARWIN AIRPORT ^b	-17.0	-15.3	-6.0	-9.3	-8.9	-0.3	0.1
ALICE SPRINGS AIRPORT	25.8	21.4	2.0	19.4	16.9	5.4	-1.8
MOUNT GAMBIER AERO	-6.1	-8.4	-0.2	-8.2	-7.4	-1.4	0.3
ROCKHAMPTON AERO	11.0	7.7	3.2	4.5	0.3	4.3	-0.2
WAGGA WAGGA AMO	-1.8	1.4	0.5	0.9	-0.5	1.4	0.1
MILDURA AIRPORT	-8.8	-11.9	0.6	-12.5	-13.2	0.6	0.3

^aOBS, observed trends; CALC, model-calculated trends. Pan evaporation rate (dE_p/dt) is given in mm a^{-2} . The modelled trend is the sum of the radiative (Rad = $dE_{p,R}/dt$) and aerodynamic (Aero = $dE_{p,A}/dt$) components per equation 4. The aerodynamic component is partitioned into components due to changing wind speed (U^*), vapour pressure deficit (D^*) and temperature (T^*) per equation 5. See auxiliary Figure S3 for data and calculations at the sites.

^bData for 1977–2004.

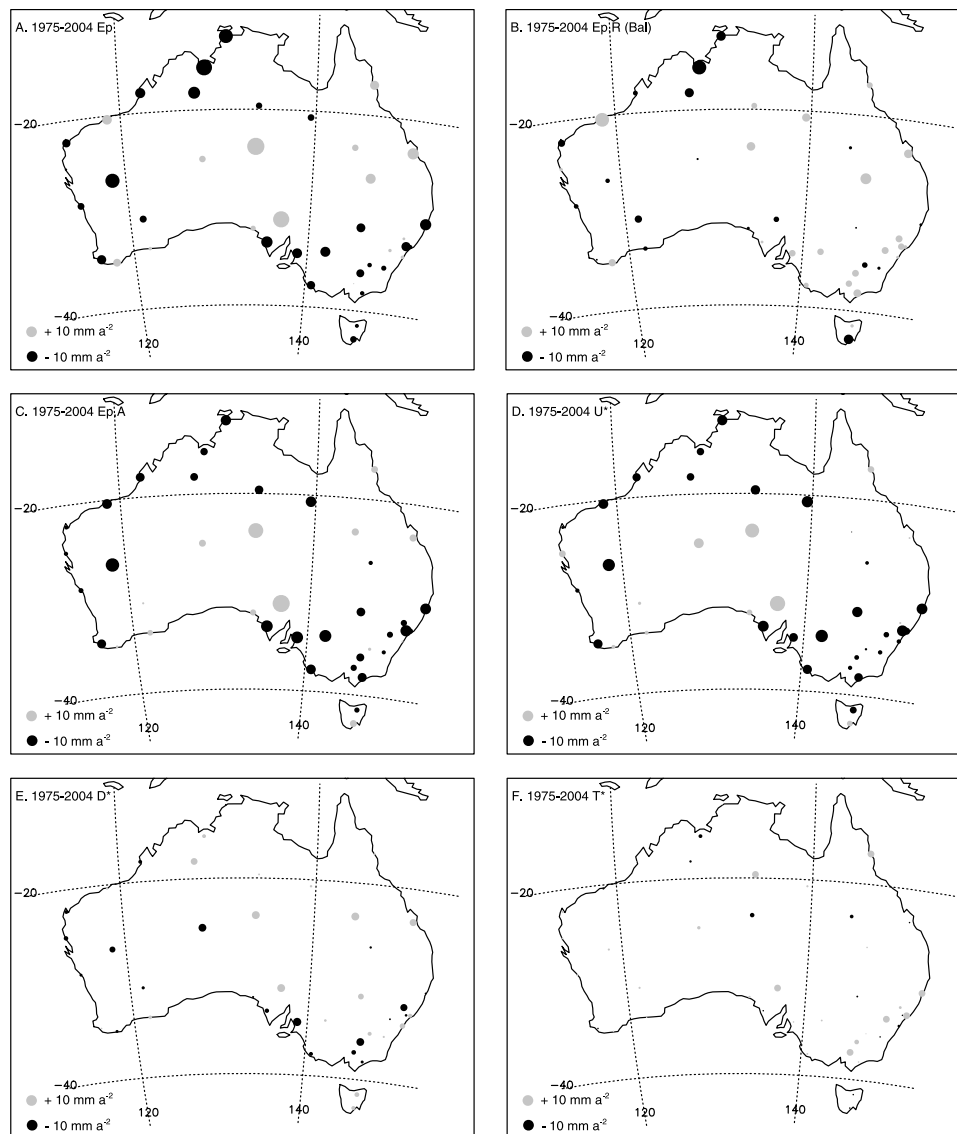


Figure 2. Trends in observed pan evaporation rate and its components at 41 sites for the period 1975–2004. (a) Observed pan evaporation rate. (b) Radiative component of pan evaporation rate calculated as the difference between Figures 2a and 2c. (c) Aerodynamic component of pan evaporation rate. The trend in the aerodynamic component is further partitioned (equation 5) into the change due to changing (d) wind speed, (e) vapour pressure deficit, and (f) air temperature. The change in each panel, averaged across all 41 sites is (a) -2.0 mm a^{-2} , (b) $+0.6 \text{ mm a}^{-2}$, (c) -2.6 mm a^{-2} , (d) -2.7 mm a^{-2} , (e) 0.0 mm a^{-2} , and (f) 0.0 mm a^{-2} . Details and trends are available for each site in auxiliary Table S1. (Note: The magnitude of the trend is scaled to the dot area per the legend.)

Table 2. Summary of Observed Changes (Represented as a Linear Trend) in Near-Surface Wind Speed (du/dt)^a

du/dt , m s ⁻¹ a ⁻¹	Location	Details	Ref.
-0.010	Australia	1975–2004, 41 sites	This study
-0.005	USA	1962–1990, 207 sites across the 48 conterminous states	<i>Hobbins</i> [2004]
-0.004	USA	1960–1990, 176 sites across the 48 conterminous states	<i>Klink</i> [1999]
-0.008	Yangtze River Catchment, China	1960–2000, 150 sites	<i>Xu et al.</i> [2006a]
-0.020	China	1969–2000, 305 sites	<i>Xu et al.</i> [2006b]
-0.010	Loess Plateau, China	1980–2000, 52 sites	<i>McVicar et al.</i> [2005]
-0.013	Tibetan Plateau	1960–2000, 101 sites	<i>Shenbin et al.</i> [2006]
-0.017	Tibetan Plateau	1966–2003, 75 sites	<i>Zhang et al.</i> [2007]
-0.013	Italy	~1955–~1996, 17 sites on Italian coast. Break point in ~1975. Trend of ~-0.026 m s ⁻¹ a ⁻¹ before and ~-0.002 m s ⁻¹ a ⁻¹ after 1975	<i>Pirazzoli and Tomasin</i> [2003]
-0.011	New Zealand	1975–2002, 5 sites	M. L. Roderick (unpublished data, 2005)
-0.017	Canada	~1950–~1990, 4 sites on west coast	<i>Tuller</i> [2004]
+0.006	Antarctica	~1960–~2000, 11 sites	<i>Turner et al.</i> [2005]

^aAll studies are based on terrestrial anemometer records.

4.2. Applying the Attribution Approach

[10] In order to test whether the approach was feasible, we first used the seven “elite” sites having complete observations for 1975–2004, where we calculated $E_{p,A}$ and $E_{p,R}$ and thereby closed the energy balance. The trends in those two components should sum to the observed E_p trend (equation 4) within error limits. The estimated uncertainty in the model calculations (24 mm mth⁻¹, Figure 1) is equivalent to an uncertainty in the trend estimate over the 30-year period of 1.8 mm a⁻² (± 1 sd). With that uncertainty, the observed and calculated trends were within 95% confidence intervals at all seven sites (Table 1).

[11] While most pan evaporation sites considered here, or anywhere, do not have radiative observations, we did have near-complete records of the aerodynamic component at each site. To apply the approach at all 41 sites, we estimated the trend in the radiative component as the difference between the trends in observations and aerodynamic components (i.e., $dE_{p,R}/dt = dE_p/dt - dE_{p,A}/dt$). The results, including the separation of the aerodynamic component into individual components (U^* , D^* , T^* per equation 5) are shown in Figure 2.

[12] Much of the trend in E_p observations (Figure 2a) was due to changes in the aerodynamic component (Figure 2c), and the majority of that was due to changes in wind speed (Figure 2d) with generally minor changes due to changes in both vapour pressure deficit and air temperature (Figures 2e and 2f). However, as expected [*Roderick and Farquhar*, 2004], there was spatial variation in the results. A notable feature is the decrease in the radiative component shown in the northwest (Figure 2b). Also of note are the two sites showing relatively large increases in E_p in the centre (Alice Springs, 133.89°E, 23.80°S) and south (Woomera, 136.81°E, 31.16°S). At Woomera there were no obvious problems with the data. At Alice Springs, the trend was very sensitive to the starting date because of very low E_p values during 1975–1978 (auxiliary Figure S3).

[13] To put the changes in perspective, the trend in D averaged over all 41 sites was -0.2 Pa a⁻¹ (auxiliary Figure S4) compared to a background average of 1205 Pa,

or less than 1% over the 30 years. In contrast, the trend in u averaged over all 41 sites was -0.01 m s⁻¹ a⁻¹ (auxiliary Figure S4) against a background average of 2.3 m s⁻¹: a reduction of 13% over the same period. The change in u was occurring more or less equally in all seasons (auxiliary Figure S5).

5. Discussion

[14] Previous research reported a trend in pan evaporation rate, averaged over 61 Australian sites for 1975–2002, of -3.3 mm a⁻² [*Roderick and Farquhar*, 2004]. This was later updated (an addendum is available from the authors) to -3.2 mm a⁻² to account for the installation of bird guards. The trend for 1975–2004 over the same 61 sites is lower at -2.4 mm a⁻² (results not shown) because of the high pan evaporation rates during the drought conditions prevailing over much of southeast Australia since 2002. For the 41 sites used here, the averaged trend for 1975–2004 was similar at -2.0 mm a⁻².

[15] Improvements could be made to the PenPan model, particularly in the calculation of the pan albedo and the treatment of incoming and outgoing long-wave irradiance. Similarly, the meteorological databases are subject to ongoing improvements [*Coughlan et al.*, 2005]. With those caveats, the model performed satisfactorily (Figure 1, Table 1) given the well-known difficulties in making long-term measurements of, and modelling, micrometeorological phenomena. According to the attribution analysis (Figure 2), the reasons for changing pan evaporation differed between sites: there was an indication of a decrease in the radiative component in northwest Australia consistent with increased rainfall and cloud cover in that region [*Smith*, 2004; *Rotstayn et al.*, 2007]. However, decreases in the aerodynamic component were more important and primarily due to decreasing wind speed. These results are consistent with recent research [*Roderick and Farquhar*, 2006; *Rayner*, 2007]. The importance of decreasing wind speed and/or radiation as a reason for decreasing pan evaporation has also been found in the USA [*Hobbins*, 2004], parts of China [*Xu*

et al., 2006a] and the Tibetan Plateau [Shenbin et al., 2006; Zhang et al., 2007].

[16] Whether the “stilling” reported here is local, i.e., attributable to changes in the immediate environment of the pans (e.g., growing trees or other obstacles progressively obstructing the air flow), or a more regional phenomenon is difficult to assess. Rayner [2007] investigated that by comparing the BoM wind observations against two alternative sources, (1) wind fields in the NCEP reanalysis, and (2) wind calculated using BoM surface air pressure observations. The results were inconclusive because the trends derived from (1) and (2) were inconsistent, and neither result was consistent with the BoM surface observations.

[17] Some of the wind speed decreases reported here are no doubt due to local effects. Alternatively, the very widespread nature of the stilling is by itself some evidence of a more robust regional effect. Indeed, the changes reported here are very similar to those reported elsewhere (Table 2). Whilst largely unanticipated in the climate change impacts community, previous analyses have predicted a slowing in the overall circulation rate in tropical regions and, presumably, a reduction in averaged wind speed in those regions with greenhouse warming [Betts, 1998; Held and Soden, 2006; Vecchi et al., 2006]. Although not strictly comparable to surface winds, the summary compiled by Lorenz and DeWeaver [2007] shows that climate models generally predict changes in zonally averaged mid-latitude wind speeds (at 850 hPa) of about -0.5 to -1.5 m s^{-1} over the 21st Century with largely complementary increases nearer the poles. This would qualitatively fit the pattern in the observations (Table 2, increase in Antarctica, decrease elsewhere). The model projections are equivalent to trends of -0.005 to -0.015 $\text{m s}^{-1} \text{a}^{-1}$ and are of the same order as the observed trends (Table 2). In contrast to the terrestrial-based anemometer records (Table 2), recently reported satellite retrievals indicate increases in oceanic wind speed averaging 0.008 $\text{m s}^{-1} \text{a}^{-1}$ for 1987–2006 [Wentz et al., 2007]. This emphasises the urgent need for research on the wind measurements and the modelling given the scientific importance as well as the widespread interest in wind power generation.

6. Conclusion

[18] When forced with radiation, temperature, humidity and wind observations, the PenPan model simulated the pan evaporation observations well. Over Australia, that approach revealed differences between sites, but on the whole, decreasing wind speed was found to be the main reason for decreasing pan evaporation. The observed decrease in wind speed, was similar to the decreases reported over other terrestrial surfaces. Our results show that the extensive world-wide network of pan evaporimeters could be used to recover information about changes in the radiative and aerodynamic drivers of evaporative demand. This would be extremely useful because there are many more pan evaporimeters than radiometers.

[19] **Acknowledgments.** We thank Alan Beswick, John Carter, Edward Linacre, David Rayner and Blair Trewin for helpful discussions and Alison Saunders for expert assistance with acquiring and processing the data. We acknowledge funding from the Managing Climate Variability Program managed by Land and Water Australia (MLR, GDF), the Aus-

tralian Greenhouse Office (LDR) and a Gary Comer Award (GDF). We acknowledge the BoM and especially the numerous BoM observers whose work formed the ultimate basis of this study.

References

- Allen, R. G., L. S. Pereira, D. Raes, and M. Smith (1998), Crop evapotranspiration: Guidelines for computing crop water requirements, *Irrig. Drainage Pap. 56*, Food and Agriculture Organization, Rome.
- Betts, A. K. (1998), Climate-convection feedbacks: Some further issues, *Clim. Change*, *39*, 35–38.
- Burn, D. H., and N. M. Hesch (2007), Trends in evaporation for the Canadian Prairies, *J. Hydrol.*, *336*, 61–73.
- Chattopadhyay, N., and M. Hulme (1997), Evaporation and potential evapotranspiration in India under conditions of recent and future climate change, *Agric. For. Meteorol.*, *87*, 55–73.
- Chen, D., G. Gao, C.-Y. Xu, J. Guo, and G. Ren (2005), Comparison of the Thornthwaite method and pan data with the standard Penman-Monteith estimates of reference evapotranspiration in China, *Clim. Res.*, *28*, 123–132.
- Coughlan, M., K. Braganza, D. Collins, D. Jones, B. Jovanovic, and B. Trewin (2005), Observed climate change in Australia, paper presented at Greenhouse 2005 Conference, Commonw. Sci. and Ind. Res. Org., Melbourne, Victoria.
- Doorenbos, J., and W. O. Pruitt (1977), Crop water requirements, *Irrig. Drainage Pap. 24*, Food and Agric. Org., Rome.
- Forgan, B. W. (2005), Australian solar and terrestrial network data, paper presented at Pan Evaporation: An Example of the Detection and Attribution of Trends in Climate Variables Workshop, Aust. Acad. of Sci., Canberra, ACT, Australia.
- Golubev, V. S., J. H. Lawrimore, P. Y. Groisman, N. A. Speranskaya, S. A. Zhuravin, M. J. Menne, T. C. Peterson, and R. W. Malone (2001), Evaporation changes over the contiguous United States and the former USSR: A reassessment, *Geophys. Res. Lett.*, *28*(13), 2665–2668.
- Groisman, P. Y., R. W. Knight, T. R. Karl, D. R. Easterling, B. Sun, and J. Lawrimore (2004), Contemporary changes of the hydrological cycle over the contiguous United States: Trends derived from in situ observations, *J. Hydrometeorol.*, *5*, 64–85.
- Held, I. M., and B. J. Soden (2006), Robust responses of the hydrological cycle to global warming, *J. Clim.*, *19*, 5686–5699.
- Hobbins, M. T. (2004), Regional evapotranspiration and pan evaporation: complementary interactions and long-term trends across the conterminous United States, Ph.D. thesis, Colo. State Univ., Fort Collins.
- Jovanovic, B., D. A. Jones, and N. Nicholls (2005), A historical monthly pan-evaporation dataset for Australia, paper presented at 16th Biennial Congress, Aust. Inst. of Phys., Canberra, ACT, Australia.
- Klink, K. (1999), Trends in mean monthly maximum and minimum surface wind speeds in the coterminous United States, 1961 to 1990, *Clim. Res.*, *13*, 193–205.
- Linacre, E. T. (1994), Estimating U.S. class A pan evaporation from few climate data, *Water Int.*, *19*, 5–14.
- Liu, B., M. Xu, M. Henderson, and W. Gong (2004), A spatial analysis of pan evaporation trends in China, 1955–2000, *J. Geophys. Res.*, *109*, D15102, doi:10.1029/2004JD004511.
- Lorenz, D. J., and E. DeWeaver (2007), The response of the extratropical hydrological cycle to global warming, *J. Clim.*, *20*, 3470–3484.
- McVicar, T. R., L. T. Li, T. G. Van Niel, M. F. Hutchinson, X. M. Mu, and Z. H. Liu (2005), Spatially distributing 21 years of monthly hydrometeorological data in China: Spatio-temporal analysis of FAO-56 crop reference evapotranspiration and pan evaporation in the context of climate change, *Land and Water Tech. Rep. 8/05*, Commonw. Sci. and Ind. Res. Org., Canberra, ACT, Australia.
- Penman, H. L. (1948), Natural evaporation from open water, bare soil and grass, *Proc. R. Soc., Ser. A*, *193*, 120–145.
- Peterson, T. C., V. S. Golubev, and P. Y. Groisman (1995), Evaporation losing its strength, *Nature*, *377*, 687–688.
- Pirazzoli, P. A., and A. Tomasin (2003), Recent near-surface wind changes in the central Mediterranean and Adriatic areas, *Int. J. Climatol.*, *23*, 963–973.
- Rayner, D. P. (2007), Wind run changes are the dominant factor affecting pan evaporation trends in Australia, *J. Clim.*, *20*, 3379–3394.
- Roderick, M. L., and G. D. Farquhar (2002), The cause of decreased pan evaporation over the past 50 years, *Science*, *298*, 1410–1411.
- Roderick, M. L., and G. D. Farquhar (2004), Changes in Australian pan evaporation from 1970 to 2002, *Int. J. Climatol.*, *24*, 1077–1090.
- Roderick, M. L., and G. D. Farquhar (2005), Changes in New Zealand pan evaporation since the 1970s, *Int. J. Climatol.*, *25*, 2031–2039.
- Roderick, M. L., and G. D. Farquhar (2006), A physical analysis of changes in Australian pan evaporation, technical report, Land and Water Australia, Canberra, ACT, Australia.

- Rotstayn, L. D., M. L. Roderick, and G. D. Farquhar (2006), A simple pan-evaporation model for analysis of climate simulations: Evaluation over Australia, *Geophys. Res. Lett.*, *33*, L17715, doi:10.1029/2006GL027114.
- Rotstayn, L. D., et al. (2007), Have Australian rainfall and cloudiness increased due to the remote effects of Asian anthropogenic aerosols?, *J. Geophys. Res.*, *112*, D09202, doi:10.1029/2006JD007712.
- Shenbin, C., L. Yunfeng, and A. Thomas (2006), Climatic change on the Tibetan plateau: Potential evapotranspiration trends from 1961–2000, *Clim. Change*, *76*, 291–319.
- Smith, I. N. (2004), An assessment of recent trends in Australian rainfall, *Aust. Meteorol. Mag.*, *53*, 163–173.
- Stanhill, G. (1997), Physics and stamp collecting: Comments arising from “The NOAA integrated surface irradiance study (ISIS)—A new surface radiation monitoring program, *Bull. Am. Meteorol. Soc.*, *78*, 2872–2873.
- Stanhill, G. (2002), Is the class A evaporation pan still the most practical and accurate meteorological method for determining irrigation water requirements?, *Agric. For. Meteorol.*, *112*, 233–236.
- Tebakari, T., J. Yoshitani, and C. Suvanpimol (2005), Time-space trend analysis in pan evaporation over Kingdom of Thailand, *J. Hydrol. Eng.*, *10*(3), 205–215.
- Thom, A. S., J. L. Thony, and M. Vauclin (1981), On the proper employment of evaporation pans and atmometers in estimating potential transpiration, *Q. J. R. Meteorol. Soc.*, *107*, 711–736.
- Thomas, A. (2000), Spatial and temporal characteristics of potential evapotranspiration trends over China, *Int. J. Climatol.*, *20*, 381–396.
- Tuller, S. E. (2004), Measured wind speed trends on the west coast of Canada, *Int. J. Climatol.*, *24*, 1359–1374.
- Turner, J., S. R. Colwell, G. J. Marshall, T. A. Lachlan-Cope, A. M. Carleton, P. D. Jones, V. Lagun, P. A. Reid, and S. Iagovkina (2005), Antarctic climate change during the last 50 years, *Int. J. Climatol.*, *25*, 279–294.
- Vecchi, G. A., B. J. Soden, A. T. Wittenberg, I. M. Held, A. Leetmaa, and M. J. Harrison (2006), Weakening of tropical Pacific atmospheric circulation due to anthropogenic forcing, *Nature*, *441*, 73–76.
- Wentz, F. J., L. Ricciardulli, K. Hilburn, and C. Mears (2007), How much more rain will global warming bring?, *Science*, *317*, 233–235.
- Wu, S., Y. Yin, D. Zheng, and Q. Yang (2006), Moisture conditions and climate trends in China during the period 1971–2000, *Int. J. Climatol.*, *26*, 193–206.
- Xu, C.-Y., L. Gong, T. Jiang, D. Chen, and V. P. Singh (2006a), Analysis of spatial distribution and temporal trend of reference evapotranspiration and pan evaporation in Changjiang (Yangtze River) catchment, *J. Hydrol.*, *327*, 81–93.
- Xu, M., C.-P. Chang, C. Fu, Y. Qi, A. Robock, D. Robinson, and H. Zhang (2006b), Steady decline of east Asian monsoon winds, 1969–2000: Evidence from direct ground measurements of wind speed, *J. Geophys. Res.*, *111*, D24111, doi:10.1029/2006JD007337.
- Zhang, Y., C. Liu, Y. Tang, and Y. Yang (2007), Trends in pan evaporation and reference and actual evapotranspiration across the Tibetan plateau, *J. Geophys. Res.*, *112*, D12110, doi:10.1029/2006JD008161.
- G. D. Farquhar, M. T. Hobbins, and M. L. Roderick, Cooperative Research Centre for Greenhouse Accounting, Environmental Biology Group, Research School of Biological Sciences, Australian National University, Canberra, ACT, 0200, Australia. (michael.roderick@anu.edu.au)
- L. D. Rotstayn, Marine and Atmospheric Research, CSIRO, Private Bag 1, Aspendale, Victoria, 3195, Australia.

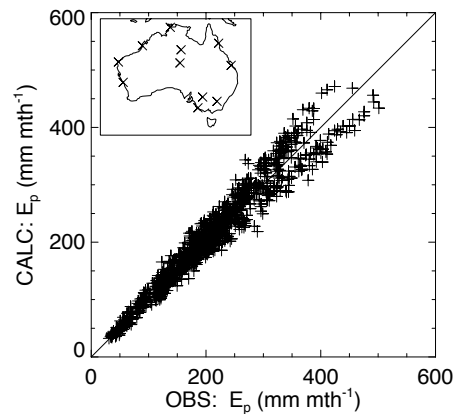
On the attribution of changing pan evaporation

Roderick, Rotstayn, Farquhar, Hobbins

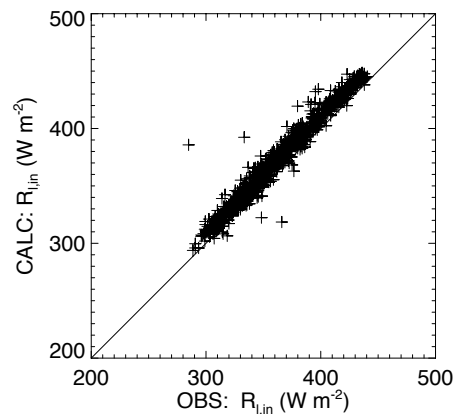
Geophysical Research Letters Article No. 2007GL031166

Auxiliary Material

August 2007



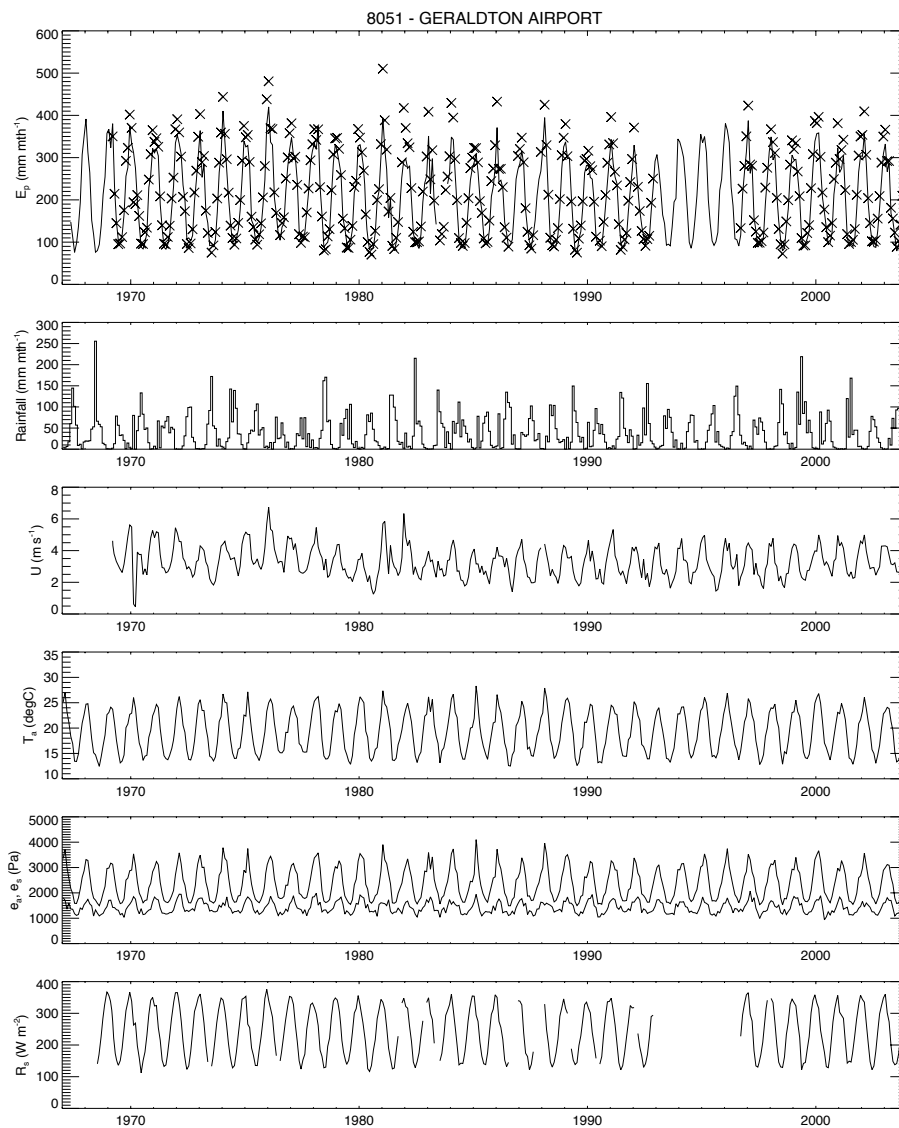
Auxiliary Figure S1 Comparison of observed and calculated pan evaporation rates. The PenPan model was forced with observations (R_s , $R_{l,in}$, T_a , e_{s2} , e_a , u). Locations (11 sites) shown in the inset. Best fit regression; $y = 0.97x + 9.6$, $R^2 = 0.95$, $n = 903$ (1:1 line shown). The RMSE is 22 mm mth^{-1} .



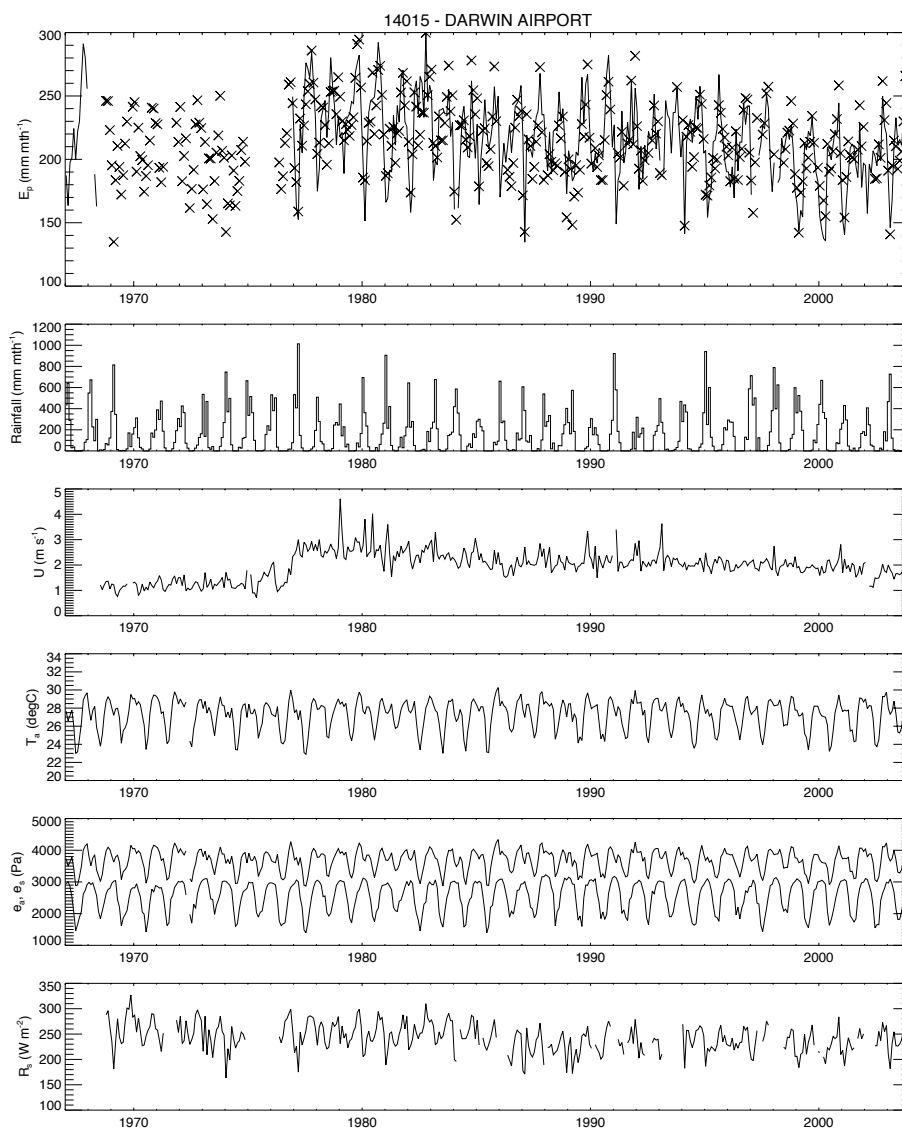
Auxiliary Figure S2 Comparison of observed and calculated incoming long wave irradiance ($R_{l,in}$). Calculations per the FAO56 model (see Eqn 6 in main text). Site locations ($n = 11$) as per Fig. A. Best fit regression; $y = 1.01x + 6.7$, $R^2 = 0.97$, $n = 916$ (1:1 line shown). The RMSE is 13 W m^{-2} .

Auxiliary Figure S3 Monthly time series for the seven “elite” sites listed in Table 1. From the top, panels show; observed (line) and PenPan based calculations (\times) of pan evaporation; rainfall; wind speed; air temperature; saturated (e_s , top) and actual (e_a , bottom) vapour pressure; global solar irradiance. The title of each plot gives the BoM station number and the name.

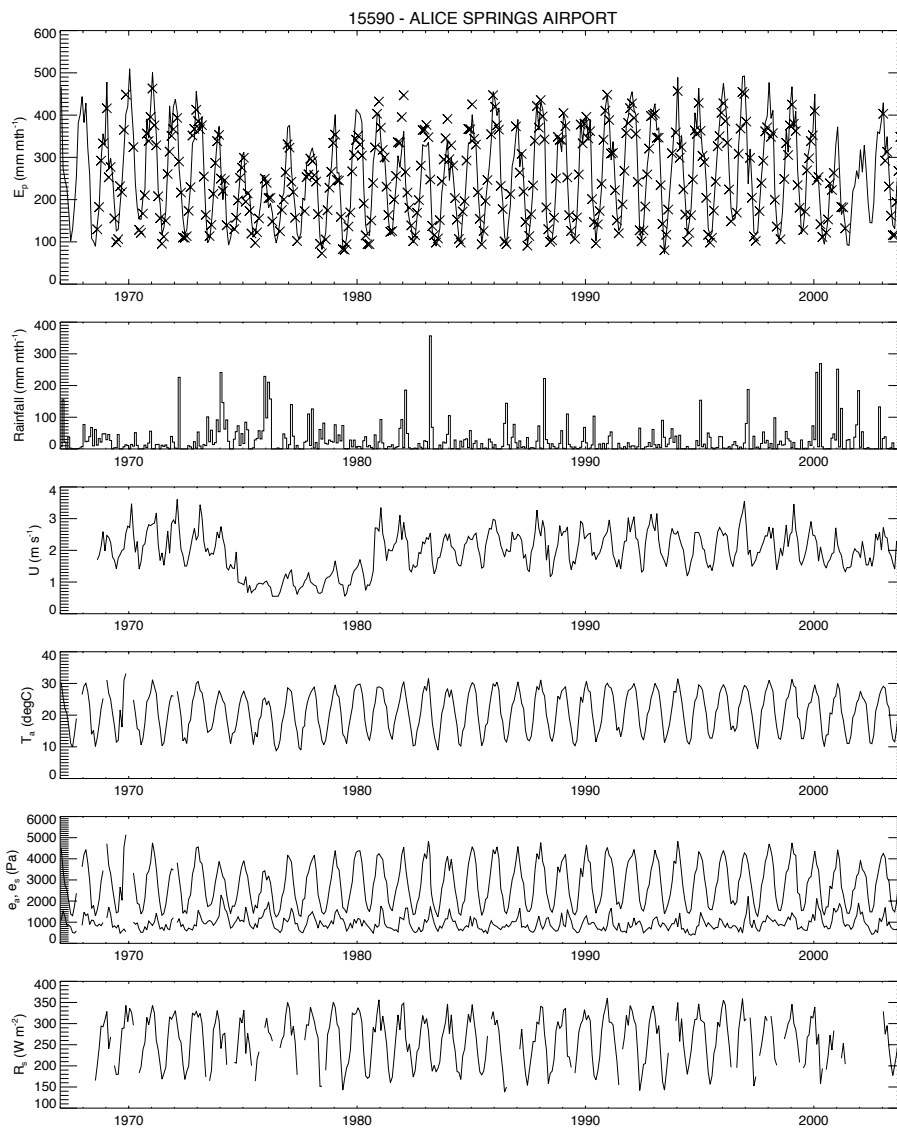
Auxiliary Figure S3a



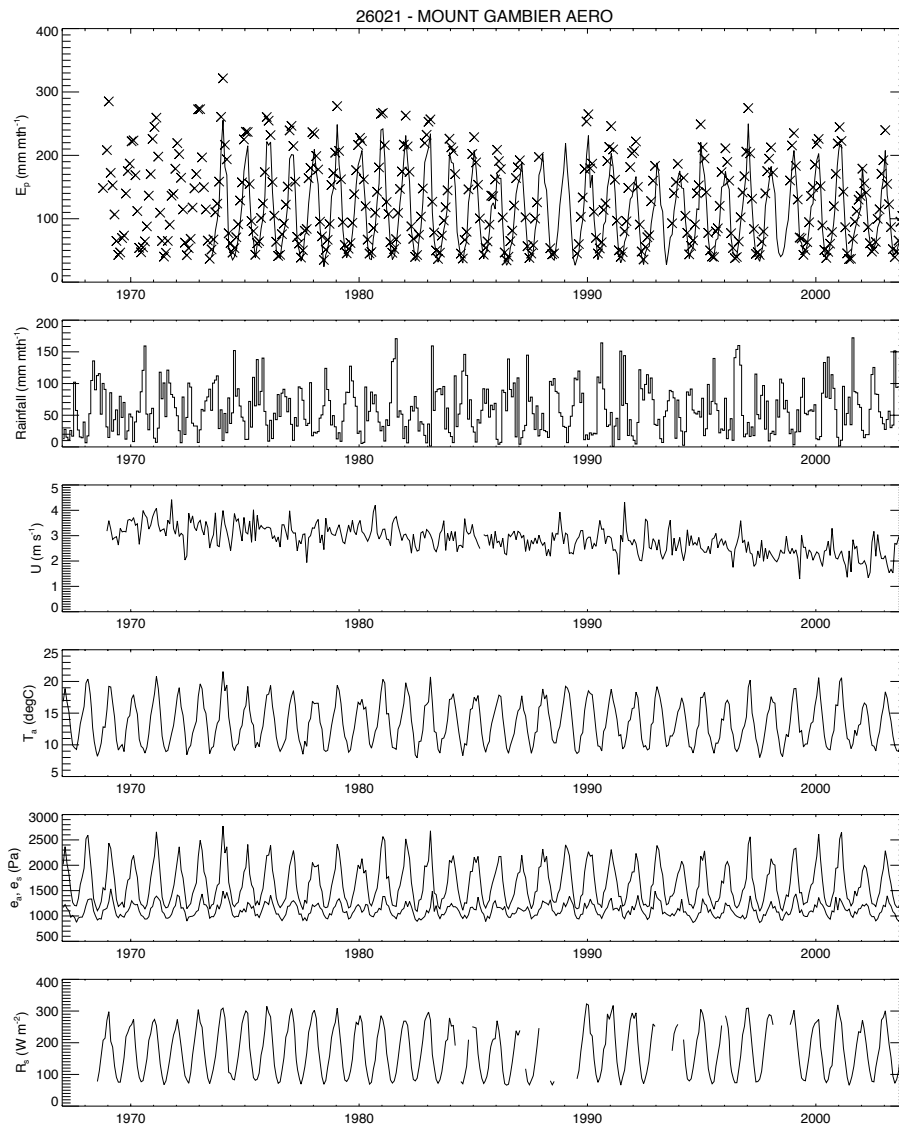
Auxiliary Figure S3b (cont'd)



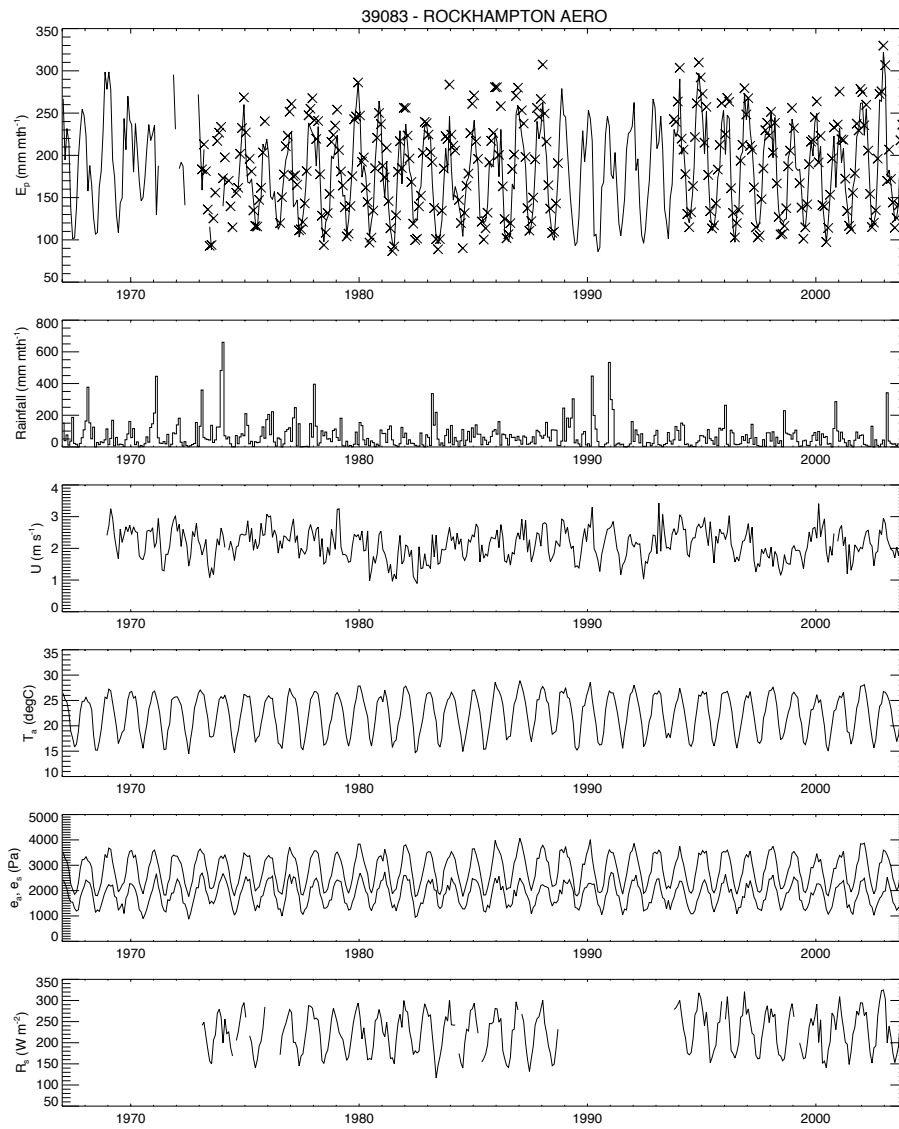
Auxiliary Figure S3c (cont'd)



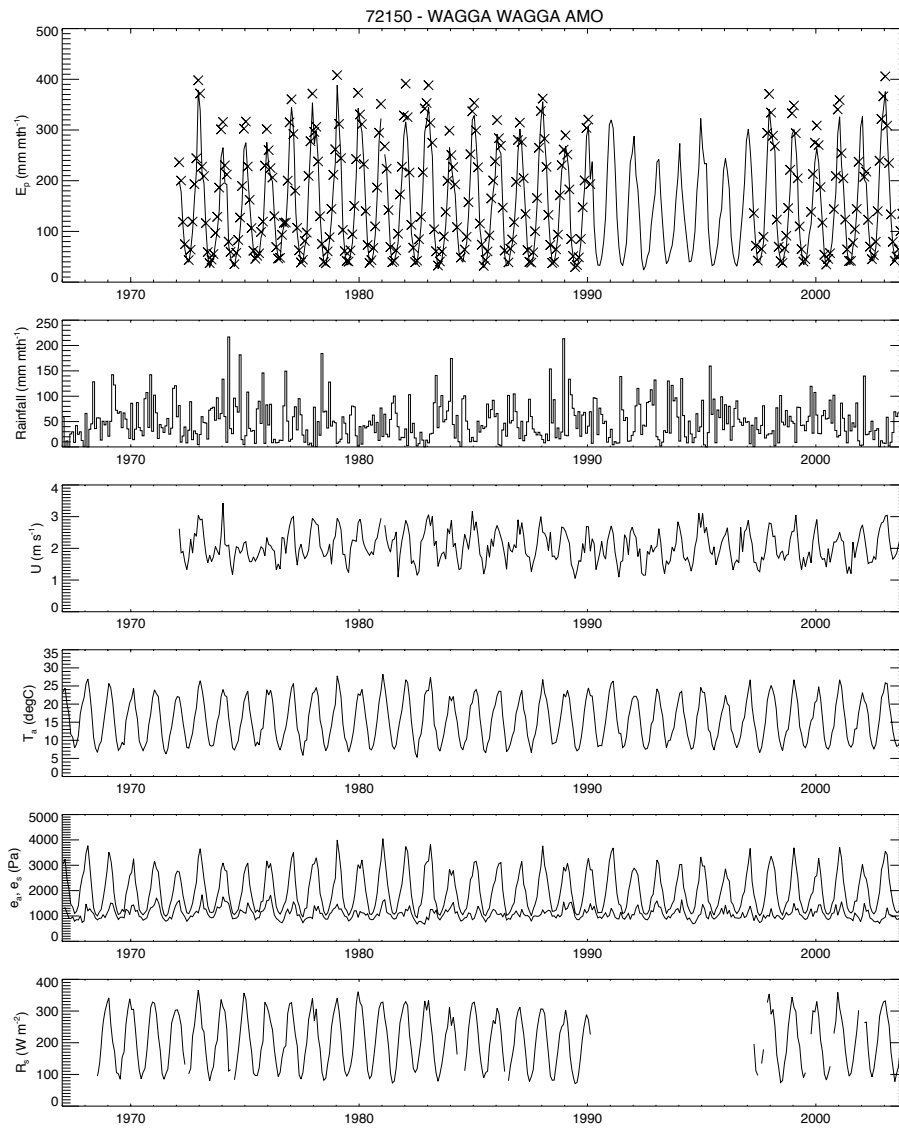
Auxiliary Figure S3d (cont'd)



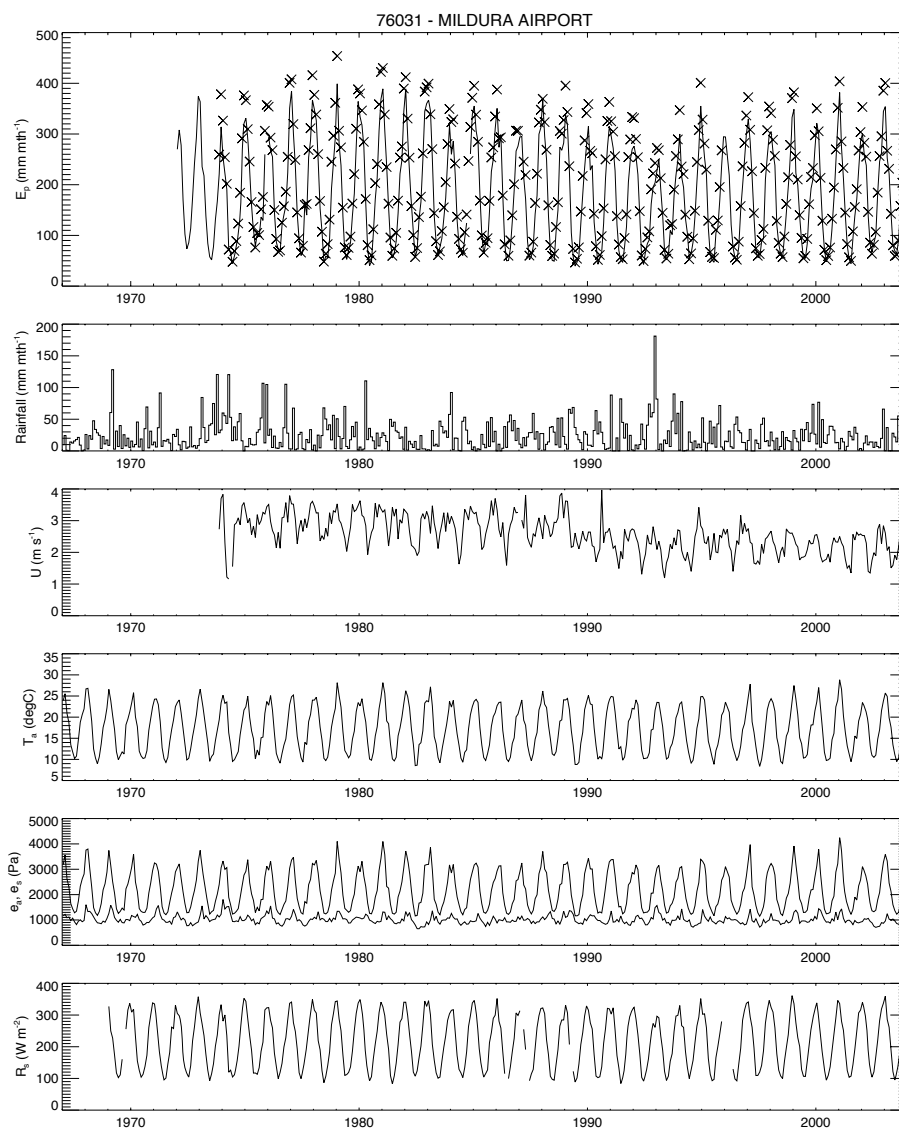
Auxiliary Figure S3e (cont'd)

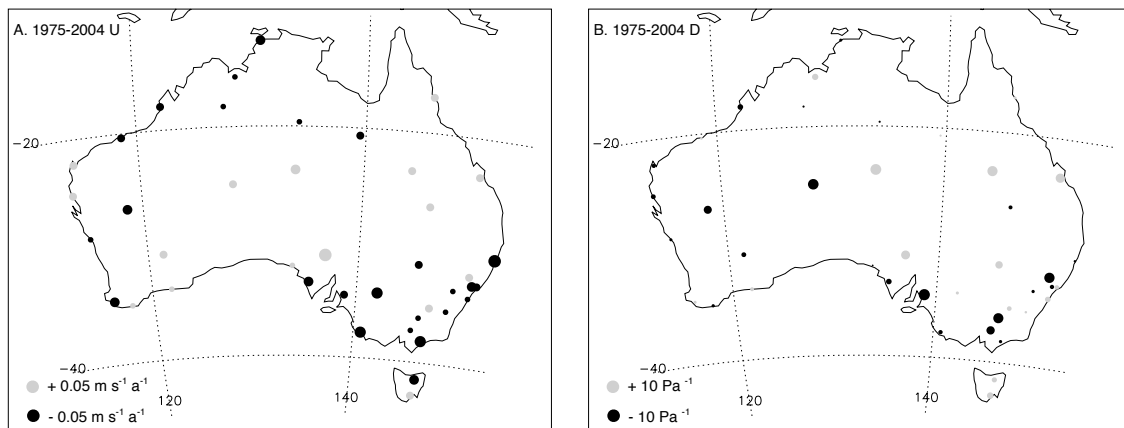


Auxiliary Figure S3f (cont'd)

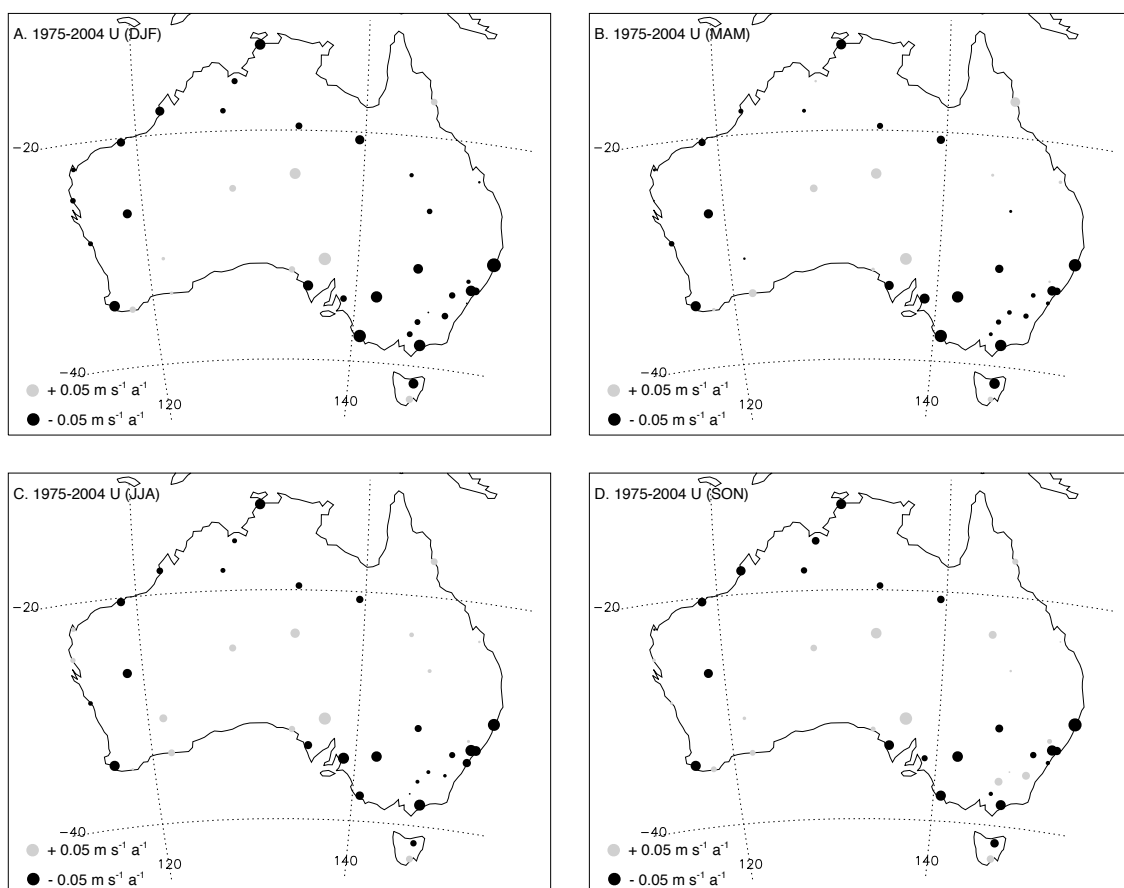


Auxiliary Figure S3g (cont'd)





Auxiliary Figure S4 Trends in (A) wind speed and (B) vapour pressure deficit at 41 sites for the period 1975-2004. The change in each panel, averaged across all 41 sites is (A) $-0.01 \text{ m s}^{-1} \text{ a}^{-1}$ and (B) -0.2 Pa a^{-1} .



Auxiliary Figure S5 Trends in wind speed at 41 sites for the period 1975-2004 in four seasons (DJF, MAM, JJA, SON). The change in each panel, averaged across all 41 sites is, (A) (DJF) $-0.01 \text{ m s}^{-1} \text{ a}^{-1}$, (B) (MAM) $-0.01 \text{ m s}^{-1} \text{ a}^{-1}$, (C) (JJA) $-0.01 \text{ m s}^{-1} \text{ a}^{-1}$, and (D) (SON) $-0.01 \text{ m s}^{-1} \text{ a}^{-1}$.

Num	Name	Lon	Lat	Ht	$\overline{E_p}$	$\frac{dE_p}{dt}$	n	$\overline{E_{p,R}}$	$\frac{dE_{p,R}}{dt}$	n	$\overline{E_{p,A}}$	$\frac{dE_{p,A}}{dt}$	n	U^*	D^*	T^*
		(deg)	(deg)	(m)	(mm a ⁻¹)	(mm a ⁻²)		(mm a ⁻¹)	(mm a ⁻²)		(mm a ⁻¹)	(mm a ⁻²)		(mm a ⁻²)	(mm a ⁻²)	(mm a ⁻²)
2012	HALLS CREEK AIRPORT	127.66	-18.23	422	3101	-12.5	355				1346	-5.3	356	-5.0	0.0	-0.5
2014	KIMBERLEY RES.STATION	128.71	-15.65	31	2758	-22.0	315				1019	-4.8	298	-4.8	1.3	-1.3
3003	BROOME AIRPORT	122.23	-17.95	7	2743	-8.9	355				984	-6.8	355	-5.9	-1.3	0.1
4032	PORT HEDLAND AIRPORT	118.63	-20.37	6	3209	8.1	354				1348	-8.4	352	-8.3	0.5	-0.4
5007	LEARMONTH AIRPORT	114.10	-22.24	5	3129	-5.9	354				1602	-1.5	353	-0.8	-1.3	0.4
6011	CARNARVON AIRPORT	113.67	-24.89	4	2647	-0.5	359				1318	-1.6	358	0.0	-1.8	0.3
7045	MEEKATHARRA AIRPORT	118.54	-26.61	517	3475	-17.5	360				1654	-15.7	360	-13.0	-3.1	0.4
8051	GERALDTON AIRPORT	114.70	-28.80	33	2425	-4.1	355	1458	0.0	298	1161	-2.2	359	-1.6	-0.8	0.3
9592	PEMBERTON	116.04	-34.45	174	1141	-7.4	321				376	-7.1	327	-7.3	0.2	-0.2
9741	ALBANY AIRPORT	117.80	-34.94	68	1406	5.3	358				565	0.7	357	1.4	-0.8	0.2
9789	ESPERANCE	121.89	-33.83	25	1648	1.1	360				698	2.8	356	1.4	1.2	0.2
12038	KALGOORLIE-BOULDER AIRPORT	121.45	-30.78	365	2614	-4.3	359				1385	0.4	351	0.9	-0.9	0.4
13017	GILES METEOROLOGICAL OFFICE	128.30	-25.03	598	3472	3.7	360				1836	4.2	347	8.4	-5.3	1.0
#14015	DARWIN AIRPORT	130.89	-12.42	30	2579	-17.0	331	1794	-6.0	305	780	-9.3	334	-8.9	-0.3	0.1
15135	TENNANT CREEK AIRPORT	134.18	-19.64	376	3965	-3.5	360				1919	-6.4	360	-7.7	0.3	0.0
15590	ALICE SPRINGS AIRPORT	133.89	-23.80	546	3057	25.8	360	1598	2.0	309	1345	19.4	360	16.9	5.4	-1.8
16001	WOOMERA AERODROME	136.81	-31.16	167	3103	22.8	357				1823	25.4	356	20.2	5.4	0.0
18012	CEDUNA AMO	133.70	-32.13	15	2248	2.4	360				1219	3.2	354	2.8	-0.4	0.5
18139	POLDA (GUM VIEW)	135.29	-33.51	37	1849	-11.2	350				977	-11.9	343	-10.3	-1.7	-0.2
23343	ROSEDALE (TURRETFIELD RESEARCH	138.83	-34.55	116	1771	-8.4	359				849	-12.2	345	-6.7	-5.9	0.2
26021	MOUNT GAMBIE AERO	140.77	-37.75	63	1292	-6.1	360	906	-0.2	320	597	-8.2	359	-7.4	-1.4	0.3
29127	MOUNT ISA AERO	139.49	-20.68	340	3107	-3.9	353				1445	-9.8	353	-11.1	0.5	0.4
31011	CAIRNS AERO	145.75	-16.87	3	2194	7.2	355				770	4.1	346	3.7	0.3	0.0
36031	LONGREACH AERO	144.28	-23.44	192	3037	3.6	360				1551	4.5	358	-0.1	5.4	-1.2
39083	ROCKHAMPTON AERO	150.48	-23.38	10	2154	11.0	360	1503	3.2	285	757	4.5	359	0.3	4.3	-0.2
44021	CHARLEVILLE AERO	146.25	-26.42	302	2584	8.7	360				1190	-1.6	351	-1.2	-0.5	0.2
48027	COBAR MO	145.83	-31.48	260	2374	-6.9	360				1109	-6.6	348	-9.2	2.9	-0.3
59040	COFFS HARBOUR MO	153.12	-30.31	5	1657	-11.0	360				518	-10.2	353	-10.1	-0.3	0.0
61078	WILLIAMTOWN RAAF	151.84	-32.79	9	1730	-1.6	359				694	-2.8	360	-4.4	1.5	0.0
61089	SCONE SCS	150.93	-32.06	216	1619	0.7	356				696	-3.4	349	0.4	-4.4	0.7
61242	CESSNOCK (NULKABA)	151.35	-32.81	62	1353	-7.4	316				559	-11	315	-10.3	-0.6	-0.2
63005	BATHURST AGRICULTURAL STATION	149.56	-33.43	713	1360	1.0	352				457	-3.2	358	-2.7	-0.3	0.0

66037	SYDNEY AIRPORT AMO	151.17	-33.94	6	1810	1.1	359				861	0.3	357	-1.7	2.6	-0.6
70014	CANBERRA AIRPORT	149.20	-35.30	578	1704	-2.3	356				616	-1.5	353	-1.7	0.4	-0.2
72150	WAGGA WAGGA AMO	147.46	-35.16	212	1787	-1.8	359	1168	0.5	265	810	0.9	359	-0.5	1.4	0.1
76031	MILDURA AIRPORT	142.08	-34.23	50	2177	-8.8	358	1250	0.6	351	1157	-12.5	359	-13.2	0.6	0.3
82039	RUTHERGLEN RESEARCH	146.51	-36.10	175	1592	-5.5	354				713	-5.5	327	-2.0	-5.3	1.9
85072	EAST SALE AIRPORT	147.13	-38.12	5	1339	-1.7	360				569	-7.1	355	-6.4	-0.8	0.2
88023	LAKE EILDON	145.91	-37.23	230	940	0.1	359				320	-3.4	338	-1.6	-1.9	0.0
91104	LAUNCESTON AIRPORT COMPARISON	147.20	-41.54	170	1267	-1.4	347				498	-2.4	356	-4.1	2.0	-0.2
94069	GROVE (COMPARISON)	147.08	-42.98	63	968	-3.7	313				321	4.2	316	2.8	1.5	-0.2

Auxiliary Table S1 Trends and averages, indicated by overbar in annual pan evaporation (E_p), and model-based calculations of the radiative ($E_{p,R}$) and aerodynamic ($E_{p,A}$) components of pan evaporation at 41 sites for the period 1975-2004 along with the number (n) of observations used in the respective calculations. U^* , D^* , T^* (see Eqn 5) are estimates of the change in the aerodynamic component due to changes in wind speed, vapour pressure deficit and temperature respectively. The trends (dE_p/dt , $dE_{p,R}/dt$, $dE_{p,A}/dt$) are the slopes of a linear regression (ordinary least squares). The trends were first calculated separately for each month, and because a linear regression was used, the annual trend at the site could be calculated from the 12 monthly trends. The advantage of this procedure is that we did not have to estimate missing data. Decomposition of the aerodynamic component ($dE_{p,A}/dt = U^* + D^* + T^*$, Eqn 5) followed the same procedure, with each of the appropriate variables held at their mean monthly values when evaluating the partial derivatives.

Data for site 14015 (Darwin Airport) is for 1977-2004.

Note 1. The BoM evaporation pans are fitted with a standardised mesh screen, called a bird-guard. During the 1970s the BoM retro-fitted bird-guards on some pans and these reduce evaporation by about 7% [Hoy and Stephens, 1979; van Dijk, 1985], so data recorded prior to bird-guard installation were reduced by 7%. Nine (of 41) sites required adjustment with the last bird-guard installed in November, 1976. The BoM bird-guard reduces the solar irradiance at the water surface by about 6% [Wallace, 1994], very close to the 7% cited above. This implies that the bird-guard reduces the radiative and aerodynamic components by about the same amount, and we reduced the PenPan model estimate of each component by 7%.

Note 2. Before 1988, the Australian R_s measurements were calibrated assuming that the mid-summer clear sky global solar irradiance (R_s) should be the same from year to year [Frick et al., 1987; Forgan, 2005]. The measurements were subsequently adjusted by the assumed sensor drift. Unfortunately, it is not possible to re-process the data as neither the original observations or the applied correction is available (B. Forgan, pers. comm.). The statistical approach used prior to 1988 assumes no trends in non-cloud atmospheric elements, of which the most important are aerosols and water vapour. The aerosol assumption is plausible in Australia but cannot be evaluated because the original measurements are unavailable. The water vapour assumption is less reasonable [Arking, 1999] but the effects should be relatively small over the 30-year period considered here. Note that changes in R_s due to changes in the amounts and optical properties of clouds will be preserved in the observations and this is expected to be the most important variable in Australia.

References

- Arking, A. (1999), The influence of clouds and water vapour on atmospheric absorption, *Geophysical Research Letters*, 26 (17), 2729-2732.
- Forgan, B. W. (2005), Australian Solar and Terrestrial Network Data, paper presented at Pan Evaporation: An example of the detection and attribution of trends in climate variables Workshop, Australian Academy of Science & Australian Greenhouse Office, Canberra, Australia, 22-23 November.
- Frick, R. A., P. J. Walsh, S. P. Rice, and M. Leadbeater (1987), Australian Solar radiation Data Handbook. Vol II. Main Report, Tech Search, University of South Australia, Adelaide.
- Hoy, R. D., and S. K. Stephens (1979), Field Study of Lake Evaporation - Analysis of Data from Phase 2 Storages and Summary of Phase 1 and 2, Australian Water Resources Council, Canberra, Australia.
- van Dijk, M. H. (1985), Reduction in evaporation due to the bird screen used in the Australian class A pan evaporation network, *Australian Meteorological Magazine*, 33, 181-183.
- Wallace, B. B. (1994), Modelling evaporation from a U.S. Weather Bureau class A pan, B. E. Hons Thesis, University of Western Australia, Perth, Australia.